Platinum(II) Metallomesogens, New External Stimuli-Responsive Photoluminescence Materials

Cristián Cuerva,[a] José A. Campo,[a] Mercedes Cano,*[a] and Carlos Lodeiro*[b,c]

Abstract: New dicatenar isoquinoline-functionalized pyrazoles [Hpz$^{R(n,n)iq}$] (R(*n*,*n*) = $C_6H_3(OC_nH_{2n+1})_2$, *n* = 4, 6, 8, 10, 12, 14, 16, 18) have been strategically designed and synthesized to induce mesomorphic and luminescence properties in their corresponding bis(isoquinolinylpyrazolate)platinum(II) complexes [Pt(pz$^{R(n,n)iq}$)$_2$]. Thermal studies reveal that all Pt^{II} compounds exhibit columnar mesophases in an exceptionally wide temperature range above 300 ºC in most cases. The photophysical behavior was also investigated in solution and in the solid state. As a consequence of the formation of Pt···Pt interactions, the weak greenish emission of the platinum derivatives turns bright orange in the mesophase. Additionally, the complexes have been found to be sensitive to a great variety of external inputs such as temperature, mechanical grinding, pressure, solvents and vapors. On this basis, they are used as dopant agents of a PVP or PPMA polymer matrix in order to achieve stimuli-responsive thin films.

Introduction

The possibility of inducing and controlling a color change in a material opens up a wide range of industrial applications in optics and optoelectronics.[1] If an external stimulus is capable of producing a change in the emissive nature of a material, then its applicability increases significantly. Currently, chromo-active materials are being investigated for their potential applications as sensors,[2] security inks,[3] data-recording devices[4] or encryption systems.[5]

As it is also known, the supramolecular assembly of square-planar Pt^{II} complexes plays a crucial role in their optical properties.[6] When the platinum atoms of two neighboring molecules are separated by a considerable distance, a greenish-blue luminescence is usually observed.[7] However, because of the strong tendency of these compounds to form aggregates *via* Pt···Pt and π···π interactions, many of them exhibit an orange-red light emission in the solid state and in solution.[8,9] The HOMO and LUMO energy levels are modified by varying the molecular packing, causing a change in the emissive response of the material.[10]

This photophysical behavior has aroused considerable interest in the last years due to its potential application in the design of smart materials. Several studies have shown that the photoluminescence of certain Pt^{II} complexes bearing azole,[11,12] bypiridine[13] and pincer[14] ligands can be tuned by controlling the way the molecules are stacked. Thus, upon mechanical grinding, for example, it is possible to induce aggregation and to generate metal–metal-to-ligand charge transfer (^{3}MMLCT) excited states, giving rise to a strong red-shifted emission. Conversely, the intermolecular Pt···Pt contacts can be broken when the sample is exposed to volatile organic compounds (VOCs), recovering the characteristic greenish emission of monomers.

A great variety of chromo-active materials based on crystalline compounds, polymers and liquid crystals have been reported to date.[15] However, less attention has been paid to metallomesogens (liquid crystals containing metals) despite they are attractive candidates on the basis of combining the fluid and ordered state of a liquid crystal with the luminescence properties of a metal.[11,16] In particular, discotic Pt^{II} metallomesogens are softer materials that would favor the establishment of intermolecular contacts between adjacent platinum centers.[10a] Due to the strong spin-orbit coupling induced by the platinum atom, these species also generate a fast intersystem crossing that allows the development of phosphorescence at room temperature. Therefore, the number of relevant works based on such systems is increasing rapidly over the last year.[17]

Following our research interest in new emissive and colorimetric liquid crystals, we describe a new family of square-planar Pt^{II} metallomesogens supported by dicatenar isoquinolinyl pyrazolate ligands, [Pt(pz$^{R(n,n)iq}$)$_2$] (pz$^{R(n,n)iq}$ = 3-(3,5-bis(alkyloxy)phenyl)-5-(isoquinolin-3-yl)pyrazolate, R(n,n) = $C_6H_3(OC_nH_{2n+1})_2$, n = 4, 6, 8, 10, 12, 14, 16, 18), which have been designed in order to increase the planarity and therefore to favor the columnar ordering of the liquid crystal phase. The introduction of the isoquinolinyl substituent has contributed to improve significantly the thermal stability of the mesophase as well as the luminescence properties, in comparison with the analogous bis(pyridylpyrazolate)platinum(II) complexes previously reported by us.[10a] On the other hand, taking into account the ease of processing of the liquid crystals and the chromo-active behavior of these Pt^{II} complexes, we have fabricated stimuli-responsive polymer thin films doped with them.

[a] C. Cuerva, Dr. J. A. Campo, Prof. M. Cano
Departamento de Química Inorgánica I
Facultad de Ciencias Químicas, Universidad Complutense de Madrid, Ciudad Universitaria, E-28040 Madrid, Spain
E-mail: mmcano@ucm.es

[b] Prof. C. Lodeiro
BIOSCOPE Research Group, UCIBIO@REQUIMTE
Chemistry Department, Faculty of Science and Technology, University NOVA of Lisbon, Caparica Campus, 2829-516 Caparica, Portugal
E-mail: cle@fct.unl.pt

[c] Prof. C. Lodeiro
PROTEOMASS Scientific Society
Rua dos Inventores, Madam Parque, Caparica Campus, 2829-516 Caparica, Portugal
E-mail: clodeiro@bioscopegroup.org

Supporting information for this article is given via a link at the end of the document.

For clarity, throughout this paper, the abbreviations ***an*** and **b*n*** are used to indicate the type of compound (pyrazole ligands [Hpz$^{R(n,n)iq}$] **a4-a18** and Pt^{II} complexes [Pt(pz$^{R(n,n)iq}$)$_2$] **b4-b18**), being *n* the number of carbon atoms in the terminal alkyl chains.

Results and Discussion

Synthesis and Characterization

Dicatenar isoquinolinyl pyrazoles [Hpz$^{R(n,n)iq}$] **a4-a18** were synthesized through a Claisen condensation between the corresponding 3,5-*n*-dialkyloxyacetophenone and ethyl isoquinoline-3-carboxylate, followed by treatment with hydrazine monohydrate. The reactions of these new species with K_2PtCl_4 in a 2:1 (ligand:metal) molar ratio yield to the new Pt^{II} complexes [Pt(pz$^{R(n,n)iq}$)$_2$] **b4-b18**, isolated as yellow solids and stable at room temperature (Scheme 1). All compounds have been fully characterized by using spectroscopic techniques (IR, ^{1}H NMR and ^{13}C NMR in selected cases) as well as CHN elemental analysis (see experimental section). Additionally, DFT calculations and NBO analysis were performed on Pt^{II} complexes in order to examine its molecular geometry and its potential intra- and intermolecular interactions.

The solid-state IR spectra of the ligands and their corresponding Pt^{II} complexes display the expected *ν*(C=N) and *ν*(C=C) bands of the isoquinoline and pyrazole fragments slightly shifted at higher frequencies (1640, 1598 cm^{-1}) in relation to those observed in the free ligand (1620, 1585 cm^{-1}). On the other hand, the characteristic *ν*(N-H) vibration of the pyrazoles can be clearly identified around 3249 cm^{-1}. By contrast, its absence in the platinum derivatives confirms the ionic nature of the ligands, which are coordinated to the metal center as isoquinolinylpyrazolates.

The ^{1}H NMR spectra of all compounds in $CDCl_3$ solution at room temperature, as well as the ^{13}C NMR spectra of **a4** and **b14** as representative examples, show the corresponding signals from the pyrazole core and the isoquinolinyl and alkyloxyphenyl substituents. A combination of 2D COSY and selective 1D NOESY spectra was required for the complete assignment of all protons. Likewise, DEPT and 2D ^{1}H-^{13}C HMQC and ^{1}H-^{13}C HMBC NMR experiments allowed the interpretation of the ^{13}C NMR spectra.

In particular for Pt^{II} complexes, the ^{1}H NMR spectra display low-intensity broad signals which could be indicative of aggregation in solution. Note that the 1-H proton signal from the isoquinolinyl group appears as a singlet at *ca.* 10.8 ppm, notably shifted to downfield with respect to that in the free ligand (~ 9.27 ppm). This fact is in good agreement with the presence of intramolecular C–H···N interactions between the two pyrazolate ligands, which should be favored by the square-planar geometry of the complexes.[10a]

As a complementary study, the ^{1}H NMR spectrum of **b8** was registered at variable concentration from 1.0 x 10^{-3} to 1.5 x 10^{-5} M. Interestingly, the broad signals observed at typical NMR concentrations are well-resolved when the sample is diluted (Figure S1), which indicates that the molecular aggregation does not occur at concentration below 5.0 x 10^{-5} M.

Figure S2 shows the structure of the Pt^{II} complexes optimized by the DFT method at the B3LYP/LanL2DZ level. The coordination around the platinum atom adopts a square-planar geometry with Pt-N1 and Pt-N3 distances of 1.991 and 2.074 Å, respectively. The pyrazolate ligands are located in a trans-disposition, so that the hydrogen atom H1 of the isoquinolinyl group of a ligand is situated near to the free N-pyrazolic atom of the other one (d(C1···N2): 3.075 Å, <(C1-H1···N2): 146.2°). This arrangement is consistent with the formation of interligand C–H···N interactions, which have been also observed in solution (see ^{1}H NMR characterization). In accordance, the calculated NBO atomic charge of the N-pyrazolic atom is -0.35 e, while the hydrogen atom of the isoquinolinyl substituent possesses a positive charge value of 0.26 e (the value found in the remaining hydrogen atoms is slightly lower of about 0.21 e). On the other hand, the isoquinoline and benzene rings show a high negative charge density with values ranging between -0.14 and -0.34 e (Figure S3). This fact suggests that the molecules could easily interact through potential intermolecular π···π interactions in the solid state.

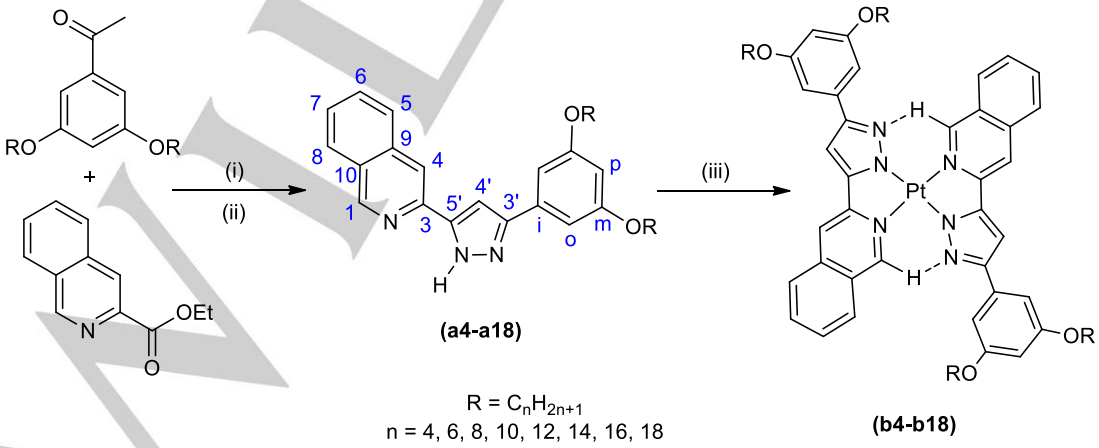

Scheme 1. Reagents and conditions: (i) NaH, refluxing in THF, 24 h; HCl; (ii) $NH_2NH_2{\cdot}H_2O$, refluxing in EtOH, 24 h; (iii) K_2PtCl_4, refluxing in EtOH, 16 h. The atom numbering used in the NMR assignment is also indicated.

Table 1. Phase behavior of Pt^{II} complexes **b4-b18**

Compound	Transitions[a]	T[b] [ºC] (ΔH/kJ mol^{-1})
b4	Cr→Col_t→Col_h→I	165 (53.0), 230 (33.0), 460
	I →Col_h→Cr	340, 111
b6	Cr→Col_h→I	93 (30.2), 450
	I→Col_h→Cr	373, 83
b8	Cr→Col_h→I	106 (58.9), 445
	I→Col_h→Cr	360, 95
b10	Cr→Col_h→I	96 (62.8), 430
	I→Col_h→Cr	370, 80
b12	Cr→Col_h→I	87 (59.0), 412
	I→Col_h→Cr	375, 75
b14	Cr→Col_h→I	88 (100.9), 412
	I→Col_h→Cr	408, 70
b16	Cr→Cr'→Cr''→Col_h→I	76 (8.3), 88, 97 (80.0)[c], 400
	I→Col_h→Cr	397, 70
b18	Cr→Cr'→Cr''→Col_h→I	66, 73, 92 (123.0)[d], 333
	I→Col_h→Cr	326, 65

[a] Cr, Cr', Cr'' = crystalline phase, Col_t = tetragonal columnar mesophase, Col_h = hexagonal columnar mesophase, I = isotropic liquid. [b] Enthalpies of the Col_h→I, I→Col_h and Col_h→Cr phase transitions were not determined due to partial decomposition; [c] Enthalpy corresponding to the overlapped phase transitions Cr'→Cr''→Col_h; [d] Enthalpy determined for the overlapped phase transitions Cr→Cr'→Cr''→Col_h.

Mesomorphism

The thermal behavior of all ligands and complexes was established by polarized light optical microscopy (POM), differential scanning calorimetry (DSC) and temperature dependent powder X-ray diffraction (XRD). Table 1 summarizes the phase transition temperatures and their associated enthalpy data for the compounds exhibiting liquid crystal properties (**b4-b18)**.

Isoquinolinyl pyrazoles **a4-a18** do not behave as liquid crystal materials, melting directly to the isotropic liquid at temperatures ranging between 78 and 162 ºC depending on the length of the alkyl chains (Table S1). The DSC thermograms show on heating a unique endothermic peak, which is attributed to the solid-isotropic liquid phase transition.

By way of contrast, the coordination of these compounds to the Pt^{II} metal center has allowed inducing enantiotropic mesomorphism in their corresponding bis(isoquinolinyl)pyrazolate platinum complexes **b4-b18**. Thus, under polarized light, the characteristic dendritic and pseudo focal-conic textures of a Col_h mesophase can be observed emerging from the isotropic liquid on cooling (Figure 1a-c). The presence of homeotropic domains evidences the columnar arrangement of the disk-like molecules, in agreement with the preferred uniaxial character of these liquid crystals. Additionally, due to the high clearing temperatures, a certain thermal decomposition is detected in all cases.

DSC studies support the above results. The Pt^{II} complexes **b6**-**b18** melt from the solid to the liquid crystal phase at *ca.* 95 - 100 ºC. These temperatures are lower than those found in some metallomesogens based on related cationic platinum compounds, so indicating that the new complexes exhibit improved liquid crystal properties.[11] For derivatives **b16** and **b18**, several endothermic peaks related to solid-solid phase transitions are additionally observed at temperatures near to the melting point.

Unlike other compounds, **b4** exhibits liquid-crystalline polymorphism, as it is clearly detected on the first heating cycle. Upon melting at 165 ºC, the thermogram shows an additional endothermic peak at 230 ºC before the clearing temperature is reached (Table 1). This mesophase transition could be also distinguished by POM in terms of a remarkable change in the mobility and in the birefringent properties of the observed fluid phase. Curiously, a similar behavior has been also reported in the literature for an analogous Pt^{II} complex bearing the tris(butoxy)phenyl-functionalized pyridylpyrazolate ligand.[9a]

By comparing the transition temperatures of all Pt^{II} compounds (Figure S4), the melting point is found to be practically similar except in **b4,** whose solid phase exhibits a high thermal stability. The increase of the van der Waals interactions among the hydrophobic tails in the complexes with longer chain length as compared with **b4** should favor the supramolecular order of the mesophase, the melting temperatures being lower. In contrast, the clearing temperature increases by decreasing the chain length, reaching values above 430 ºC for the complexes with the shortest alkyl chains. As a consequence of the increase of the mobility, the presence of long terminal chains constitutes a drawback to achieve intermolecular interactions that stabilize the mesophase. On the basis of these results, **b12** and **b14** show the best liquid crystal properties while the complex **b6** exhibits the highest mesophase stability range.

Small-angle powder XRD analysis at variable temperature allowed unequivocally identifying the liquid crystal phases established by POM and DSC. The studies were carried out on heating for compounds **b4**, **b6** and **b12**, selected as representative examples of the Pt^{II} complexes. Results are summarized in Table 2.

The diffractograms of **b4** display well-defined peaks with a *d*-spacing ratio of 1 : 1/√2 : 1/√4 : 1/√5 : 1/√8 : 1/√9 : 1/√10 : 1/√13 : 1/√17 at a temperature range from 170 to 220 ºC, which can be attributed to the characteristic reflections of a two-dimensional tetragonal lattice (a = 15.6 Å) (Figure 1d).[18] In the wide-angle region, no diffraction peak due to the stacking of consecutive discotic units is observed, this fact suggesting the

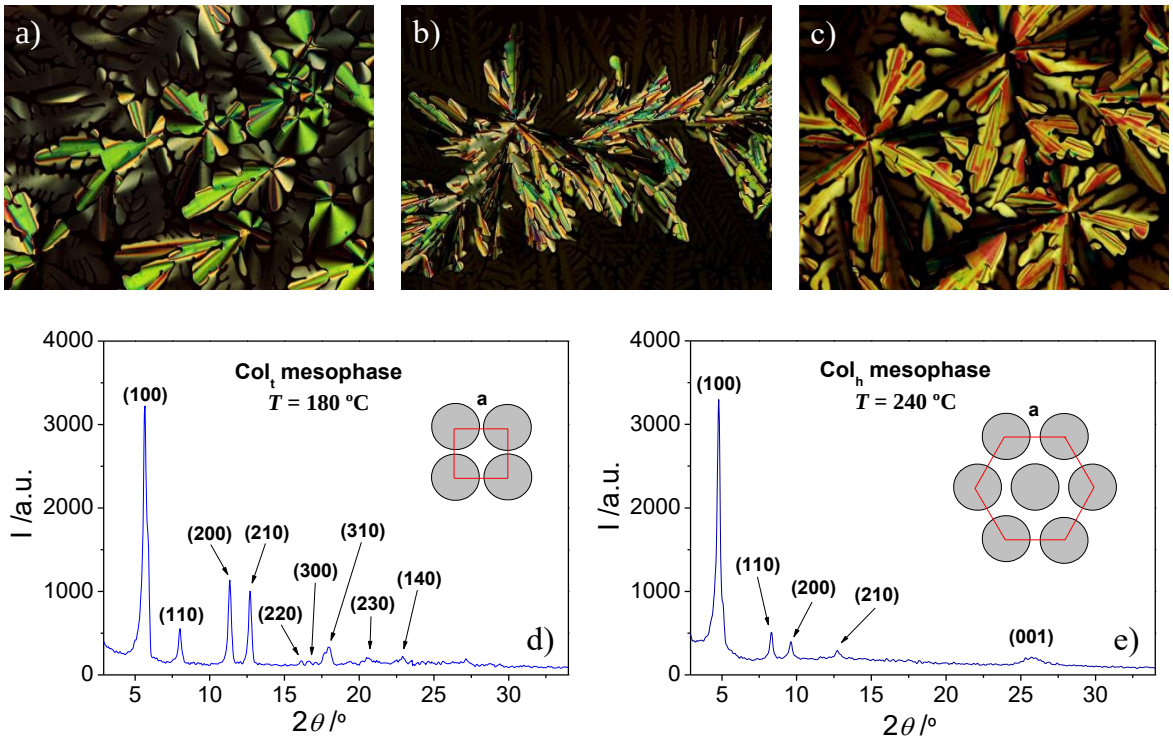

Figure 1. Characterization of the liquid-crystalline phases: polarized light optical microphotographs of the Col_h mesophases observed on cooling of (a) $[Pt(pz^{R(10,10)iq})_2]$ b10 at 244 ºC and (b,c) $[Pt(pz^{R(12,12)iq})_2]$ b12 at 348 and 306 ºC, respectively. Powder X-Ray diffraction pattern of $[Pt(pz^{R(4,4)iq})_2]$ b4 at (d) 180 ºC and (e) 240 ºC.

formation of a disordered tetragonal columnar mesophase. By increasing the temperature, the XRD diffractograms change and they show a new signal pattern composed of four peaks in a 1 : 1/√3 : 1/√4 : 1/√7 *d*-spacing ratio that can be indexed to the (100), (110), (200) and (210) reflections of a hexagonal lattice (*a* = 21.3 Å). An additional peak corresponding to the intracolumnar distance is also observed at 3.4 Å and attributed to the (001) reflection (Figure 1e). From the above results, we proposed that the disordered Col_t mesophase is thermally transformed in the more stable Col_h mesophase, which in turn exhibits a high long-range order along the columns.

On the other hand, the diffractograms of **b6** and **b12** show the characteristic (100), (110), (200), (210) and (001) reflections of an ordered hexagonal columnar phase in all range of existence of the mesophase (Figure S5). Lattice constants are similar to that of the Col_h mesophase of **b4**, although slightly higher due to the increase of the alkyl chains length. Likewise, the molecular volume and cross-section area have been calculated assuming a density of 1.1 – 1.2 g/cm^3. The results are consistent with the experimental intracolumnar distance and they are in agreement with the columnar stacking proposed in which one single Pt^{II} complex constitutes the elementary discotic unit.

Photophysical Characterization

The photophysical characterization of the pyrazole ligands **a4 – a18** and their corresponding Pt^{II} complexes **b4 – b14** was carried out at 298 K in CH_2Cl_2 solution and in the solid state. The low solubility of **b16** and **b18** did prevent to perform their characterization in solution. Because the absorption and emission spectra of compounds of each family exhibit a similar pattern, only those of **a8** and **b4** are depicted as representative examples in Figure 2. All data are summarized in Table 3.

The UV-Vis spectra of the isoquinolinyl pyrazoles exhibit a band in the higher-energy region (240 – 350 nm) attributed to the π-π* transitions of the isoquinolinyl and pyrazole moieties.[19] Their corresponding emission band appears at *ca*. 376 nm being slightly red-shifted in the solid state, except for the ligands **a8**, **a10** and **a14**, in which the emission maximum is located at *ca*. 373 nm.

The absorption spectra of Pt^{II} complexes show the corresponding band of the intraligand (IL) pyrazolate (π) → isoquinoline (π*) transitions in the wavelength range from 250 to 390 nm. At lower frequencies, it is also possible to observe a band with a relatively small molar extinction coefficient of the order of about 10^3 L mol^{-1} cm^{-1}, which can be assigned to singlet and triplet metal-to-ligand charge transfers (MLCTs) mixed with a certain degree of the IL π-π* transition.[8]

Concerning the emission, all compounds exhibit the characteristic greenish luminescence of the monomeric species in solution (λ ≈ 527, 560 nm), with a short lifetime of *ca.* 0.11-0.14 ns and other one longer ranging 2.81-3.43 ns. The

Table 1. X-Ray diffraction data

	2θ [º]	d_{meas}[a] [Å]	d_{calc}[b] [Å]	[*hkl*][c]	Parameters[d]
b4	5.6	15.6	15.6	100	Col_t
	8.0	11.1	11.0	110	T = 180 ºC a = 15.6 Å
	11.3	7.8	7.8	200	S_{col} = 243 Å^2
	12.7	7.0	7.0	210	
	16.1	5.5	5.5	220	
	16.6	5.3	5.2	300	
	18.0	4.9	4.9	310	
	20.5	4.3	4.3	230	
	22.9	3.9	3.8	140	
	4.8	18.4	18.4	100	Col_h
	8.3	10.6	10.6	110	T = 240 ºC a = 21.3 Å
	9.6	9.2	9.2	200	V_{mol} = 1417 Å^3 S_{col} = 393 Å^2
	12.7	7.0	6.9	210	h = 3.6 Å
	25.9	3.4	-	001	
b6	4.4	20.0	20.0	100	Col_h
	7.6	11.6	11.5	110	T = 180 ºC a = 23.2 Å
	8.8	10.0	10.0	200	V_{mol} = 1573 Å^3 S_{col} = 466 Å^2
	11.4	7.7	7.6	210	h = 3.4 Å
	26.0	3.4	-	001	
b12	3.7	23.6	23.6	100	Col_h
	6.4	13.8	13.6	110	T = 200 ºC a = 27.6 Å
	7.4	12.0	11.8	200	V_{mol} = 2224 Å^3 S_{col} = 660 Å^2
	9.7	9.1	8.9	210	h = 3.4 Å
	26.0	3.4	-	001	
	18.0	4.9	-	-	

[a], [b] d_{meas} and d_{calc} are the measured and calculated diffraction spacings. [c] [*hkl*] are the Miller indices of the reflections. [d] Molecular volume: $V_{mol} = M_w/(N_A \cdot \rho)$; where M_w is the molecular weight, N_A is Avogadro's number and ρ is the density (~ 1.1-1.2 g·cm^{-3}). For tetragonal columnar phases: lattice constant $a = d_{100}$; columnar cross-section area $S_{col} = a^2$. For hexagonal columnar phases: lattice constant $a = 2[\Sigma d_{hk}\sqrt{(h^2 + k^2 + hk)}]/\sqrt{3}N_{hk}$, where N_{hk} is the number of *hk0* reflections; columnar cross-section area $S_{col} = (\sqrt{3})a^2/2$; intracolumnar distance $h = V_{mol}/S_{col}$.

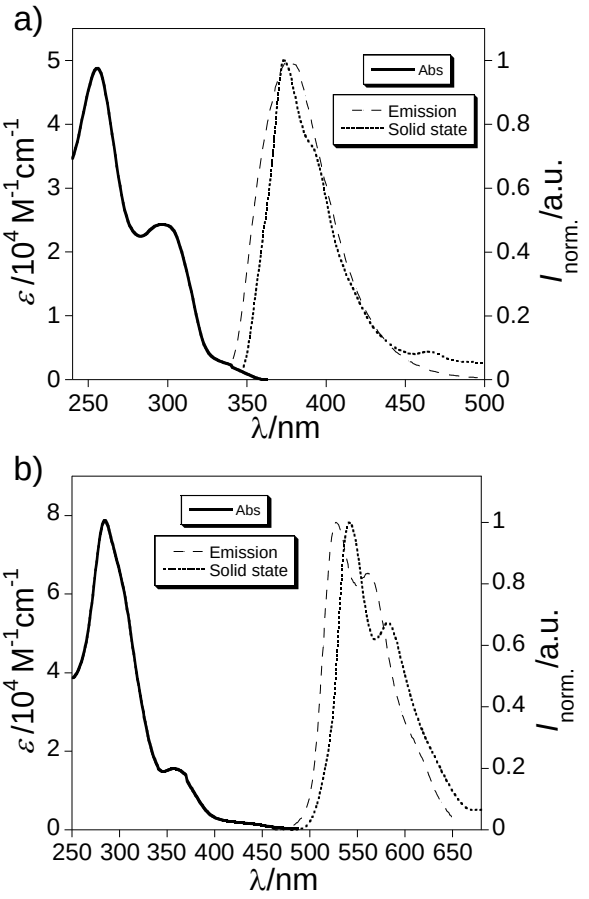

Figure 2. UV-Vis absorption and normalized emission spectra in CH_2Cl_2 solution (1 x 10^{-5} M) and in the solid state of (a) [Hpz$^{R(8,8)iq}$] a8 and (b) [Pt(pz$^{R(4,4)iq}$)$_2$] b4 at 298 K.

biexponential decay can be attributed to MLCTs simultaneously originated in both the singlet and triplet manifolds. It is interesting to note that the slight red-shift observed in the solid state (λ ≈ 541, 584 nm) can be due to the presence of π···π interactions between monomers. In fact, the high planarity of these Pt^{II} complexes also favors the establishment of short contacts in solution (see ^{1}H NMR characterization).

As it can be observed in Figure S6, by increasing the concentration of the complex **b8** from 1 x 10^{-5} to 5 x 10^{-4} M, the luminescence maximum at 528 nm disappears and results in a broad band centered around 600 nm. This red-shifted emission is fundamentally originated from a triplet metal–metal-to-ligand charge transfer (^{3}MMLCT) state and evidences the formation of aggregates *via* Pt···Pt interactions.[10a-c] However, the aggregation is not complete and a broad shoulder from the monomeric form is detected about 540 nm. In this context, the luminescence lifetime of the most soluble complex, **b4,** was determined in CH_2Cl_2 solution at very high concentration (10^{-3} M). As expected, two independent emission lifetimes of 0.12 and 99 ns could be measured in accordance with the presence of the Pt^{II} complex in both monomeric and aggregated forms, respectively.

Table 3. Absorption (λ_{abs}^{max}) and emission (λ_{em}^{max}, $\lambda_{em(solid)}^{max}$) maxima in nm, molar absorption coefficients (ε) in L mol^{-1} cm^{-1} and luminescence quantum yields (Φ_F) for ligands and complexes in CH_2Cl_2 solution and in the solid state at 298 K.

Compound		λ_{abs}^{max} (ε/10^4)[a]	λ_{em}^{max} [a]	$\lambda_{em\ (solid)}^{max}$ [a]	$\Delta\lambda$[b]	Φ_F[c]
[Hpz$^{R(n,n)iq}$]	**a4**	255 (4.3), 297 (2.1)	376	416	79	0.09
	a6	255 (4.4), 297 (2.1)	374	393	77	0.07
	a8	255 (4.9), 297 (2.4)	376	373, 392	79	0.07
	a10	255 (3.1), 297 (1.5)	376	374, 393	79	0.09
	a12	255 (3.4), 297 (1.7)	376	383	79	0.06
	a14	255 (3.2), 298 (1.5)	374	372, 389	76	0.09
	a16	255 (3.8), 297 (1.8)	374	387	77	0.06
	a18	255 (3.2), 297 (1.6)	376	388	79	0.05
[Pt(pz$^{R(n,n)iq}$)$_2$]	**b4**	285 (7.8), 358 (1.6), 435 (0.2)	527, 561	541, 583	92	0.02
	b6	284 (6.6), 356 (1.3), 435 (0.4)	526, 561	546, 584	91	0.01
	b8	285 (10.7), 358 (2.2), 434 (0.7)	528, 560	546, 585	94	0.02
	b10	284 (9.8), 357 (1.8), 434 (0.3)	528, 559	541, 583	94	0.02
	b12	284 (9.2), 356 (1.6), 435 (0.2)	526, 561	541, 587	91	0.03
	b14	284 (7.1), 358 (1.3), 435 (0.3)	525, 559	540, 581	90	0.06

[a] Estimated error: ± 1 nm. [b] Stokes shift. [c] Estimated error: ± 5 %.

Thermo-, Mechano- and Vapochromic Behaviors

In order to investigate the photophysical properties of the Pt^{II} complexes **b4-b14** in the liquid crystal state, variable-temperature luminescence studies were performed from the solid to the mesophase, and vice versa. In general terms, the spectral profile was found to be similar in all compounds. On heating, the monomer emission with the maximum around 541 nm is quenched by increasing the temperature, and then a new red-shifted band with a strong luminescence intensity appears at *ca*. 607 nm (Figure 3). Note that this feature is directly related with the solid – liquid crystal phase transition. In fact, the emission change occurs during the formation of the mesophase, and therefore at a different temperature for each complex. As it was established by XRD analysis, the intracolumar distance in the Col$_h$ mesophase is 3.4 Å, value consistent with the presence of Pt(d$_z^2$)···Pt(d$_z^2$) and π···π interactions. With this in mind, the orange emission in the liquid crystal phase could be tentatively attributed to a ^{3}MMLCT excited state induced by the formation of Pt···Pt aggregates in the mesophase. This can be rather surprising because aggregation processes usually occurs at low temperature. However, the absence of the MMLCT emission in the solid state at room temperature suggests that the Pt^{II} molecules are arranged in a tilted stacking with a considerable Pt-Pt distance, as it has been found in related platinum derivatives.[8,10a,12a,19] Thus, by increasing the temperature, the motion of the molecules should favor the formation of Pt^{II} aggregates in the liquid crystal phase, so enhancing the emission rather than quenching it.[9i] On the other hand, this strong luminescence decreases upon heating at high temperatures due to thermally activated non-radiative processes. In agreement with them, a weak intensity ^{3}MMLCT band was observed only for complex **b4** as a consequence of its high melting point (Figure S7).

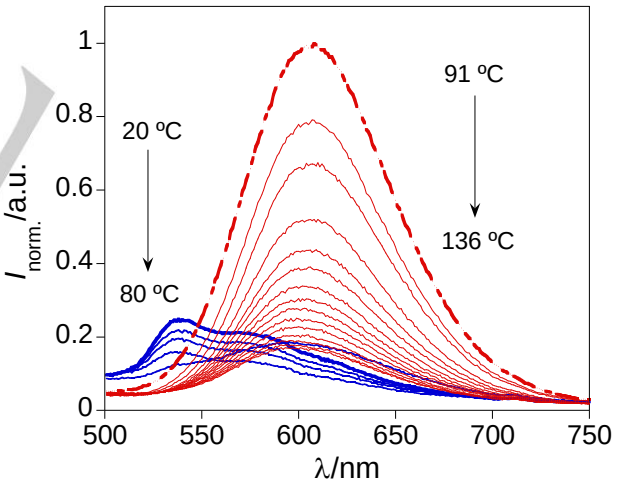

Figure 3. Photoluminescence spectra of complex [Pt(pz$^{R(14,14)iq}$)$_2$] **b14** at variable temperature on heating.

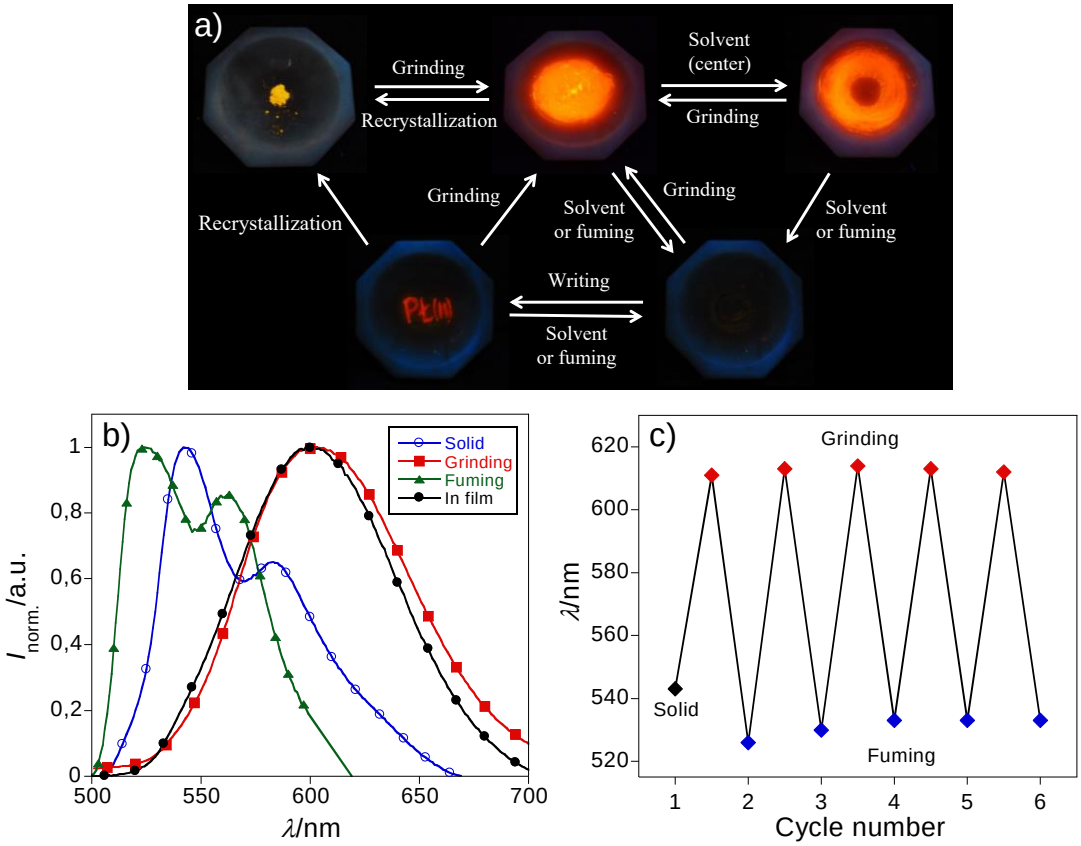

Figure 4. a) Reversible mechanochromic behavior of complex [Pt($pz^{R(4,4)iq}$)$_2$] **b4**. The images were obtained under UV radiation (λ_{exc} = 365 nm). b) Normalized emission spectra of [Pt($pz^{R(4,4)iq}$)$_2$] **b4** in film, upon grinding with a pestle and after dichloromethane fuming process. c) Grinding/fuming cycles showing the reversibility of the mechanochromic properties of **b4**.

On cooling from the liquid crystal phase, the emission of all Pt^{II} complexes is practically restored. As shown in Figure S8 for **b14**, the maximum peak centered at *ca.* 615 nm evidences that the columnar organization of the mesophase is maintained after the solidification process, so achieving a significant enhancement of the initial greenish solid-state emission.

To further explore the influence of Pt···Pt interactions on the luminescence properties, the emissive response of these platinum derivatives has been also evaluated by applying mechanical and chemical external stimuli. Upon grinding the crystalline solid with a pestle, the green-yellow emission that the complexes exhibit in the solid state turns bright orange in just a few seconds (Figure 4a). The mechanical agitation produces a displacement of the Pt^{II} monomers favoring the formation of aggregates through effective Pt···Pt interactions and leading to ^{3}MMLCT transitions. A similar behavior is also observed in thin *film*. By evaporation of the solvent, monomers tend to align along the axial axis of each molecule, so establishing short contacts between the metal centers. In both cases the mechanochromic shift response is found to be of about 60 nm (Figure 4b).

Nevertheless, it is possible to recover again the greenish emission breaking the intermolecular Pt···Pt contacts by adding

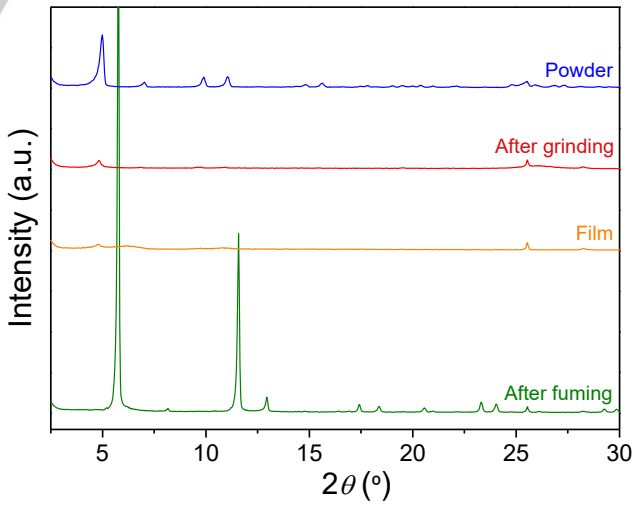

Figure 5. XRD diffractograms of **b4** as prepared (blue), upon grinding (red), in film (orange) and after fuming (green).

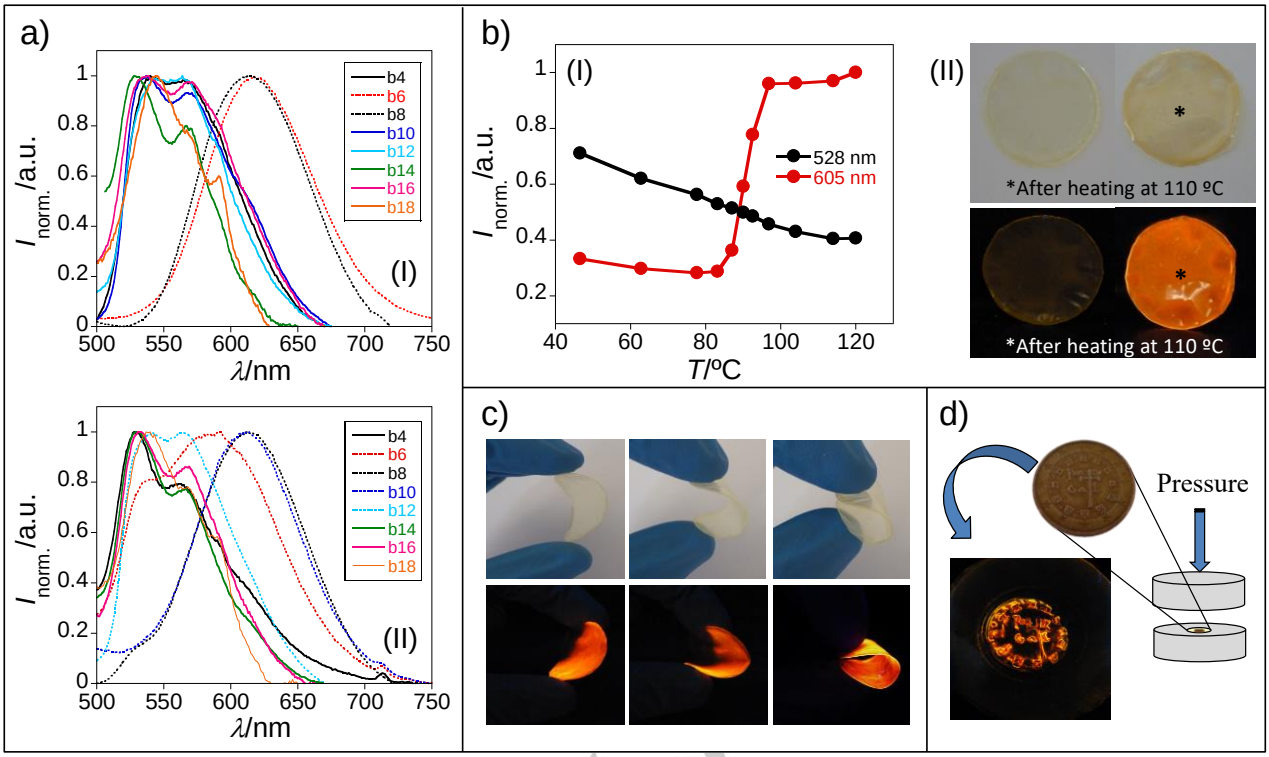

Figure 6. Photoluminescence behavior of stimuli-responsive polymer thin films. a) Normalized emission spectra of PMMA (I) and PVP (II) thin films doped with the Pt^{II} complexes **b4**-**b18**. b) Thermochromic properties of the PMMA films. (I) Normalized emission intensity of the PMMA/**b14** film as a function of the temperature, read at 528 and 605 nm. (II) Images of PMMA/**b14** polymer film before and after heating at 110 ºC on a hot surface upon ambient and UV light (λ_{exc} = 365 nm). c) Images taken folding the PMMA/**b14** polymer before and after heating it at temperatures above 120 ºC. (d) Coin imprint in a PMMA film doped with the complex $[Pt(pz^{R(16,16)iq})_2]$ **b16**.

dichloromethane or by exposure to their vapors. As depicted in Figure 4b, after treatment of the orange-emitting sample with vapor of CH_2Cl_2, the emission maximum changes from 605 to 526 nm. This mechano- and vapochromic behavior can be reproduced during successive cycles without causing the degradation of the sample (Figure 4c and S9).

To understand the possible changes of the molecular packing during a grinding/fuming cycle and confirm that the red-shift emission is originated by the formation of aggregates, XRD studies were carried out in **b4**. As it is shown in Figure 5, the well-resolved diffraction peaks of the powder sample become very weak and broad upon grinding, which is indicative of the formation of partially amorphous aggregates.[14d] A similar XRD pattern was also obtained in thin *film*. In contrast, after fuming with CH_2Cl_2, the orange amorphous phase is converted in a crystalline solid as evidenced from the intense, sharp and shifted diffractions peaks. This solid exhibits again a similar greenish emission than that of the initial powder one (see Figure 4).

The mechanochromic properties were similar for all complexes regardless of the alkyl chain length. It suggests that the Pt···Pt interactions are determinant to favor the columnar stacking of the molecules, while the intermolecular interactions between the alkyl chains do not significantly affect to the stimuli-responsive properties of these materials. Additionally, the luminescence writable ability of the Pt^{II} compounds was proved to write with a spatula the symbol “Pt(II)” on the recovered yellow solid (Figure 4a). The new complexes have a great potential as write-read-erase materials for use in the fabrication of memory devices.

Stimuli-responsive Polymer Thin Films

Films of polymethylmethacrylate (PMMA) and polyvinylpyrrolidone (PVP) doped with a 1% of the Pt^{II} metallomesogens were prepared by the solvent-casting method. Figure 6a shows the normalized emission spectra of the films registered at room temperature. In most cases, Pt^{II}-based polymers exhibit a weak greenish luminescence (λ ≈ 528, 566 nm), which can be attributed to the monomer form. However, the emission spectra of the PMMA films doped with **b6** and **b8** display the broad band at 614 nm corresponding to the formation of Pt···Pt aggregates. This emission is also observed in PVP thin films of the compounds **b6**, **b8** and **b10**, but in these cases the presence of a shoulder at 528 nm evidences an incomplete aggregation.

On the basis of the above results, we were interested in testing the possibility of producing the aggregation of the Pt^{II} complexes in the greenish-emitting polymers by application of an external stimulus, as it was proved for pure metallomesogens. The flexibility provided by the polymer in combination with the

chromic response of the complex might be useful to develop stimuli-responsive advanced materials. In this context, the PMMA and PVP polymers doped with **b14** (chosen as representative examples) were subjected to a continuous heating in order to evaluate its thermochromic behavior. The aggregation of the molecules was detected around 87 and 100 ºC, respectively, when the greenish emission attributed to the monomer form (λ = 528 nm) turned bright orange (λ = 605 nm) (Figure 6b and S10). Upon cooling again the film at room temperature, the photoluminescence did not show significant changes, which evidences that the aggregation is irreversible. In addition, the physical properties of the polymer were not affected by the temperature, the material remaining the same initial flexibility and mechanical strength (Figure 6c).

On the other hand, the polymer film PMMA/**b16** was scraped with a spatula to induce the formation of Pt-aggregates. Immediately, the color change from green to bright orange was detected in the modified region. However, this transformation might be related to the increase of temperature produced on the film as a consequence of the mechanical agitation. Then, to decrease this possible effect, we apply pressure on a coin placed over the polymer for a few minutes. As shown in Figure 6d, the aggregation only occurred in those regions of the polymer that were in direct contact with the coin surface, so creating an exact copy of its relief.

Conclusions

A new family of isoquinolinyl pyrazole compounds [Hpz$^{R(n,n)iq}$] and their corresponding multifunctional Pt^{II} derivatives of the type [Pt(pz$^{R(n,n)iq}$)$_2$] have been synthesized and their liquid crystal and luminescence properties explored. All complexes behave as mesomorphic materials exhibiting highly stable mesophases in a temperature range above 241 ºC in all cases. In particular, XRD analysis of the Pt^{II} complex with four carbon atoms at the alkyl chains reveals the formation of a tetragonal mesophase at 165 ºC, which is transformed into a more stable hexagonal columnar one at higher temperature. The remaining complexes show a unique liquid-crystalline phase identified as a hexagonal columnar mesophase.

The greenish emission that these square-planar Pt^{II} complexes exhibit in the solid state turns bright orange at the mesophase temperature. This color change is related to the formation of molecular aggregates through Pt···Pt interactions, which induce metal-metal-to-ligand charge transfer (^{3}MMLCT) excited states. A similar behavior is also observed after grinding the crystalline solid with a pestle or scraping with a spatula. Interestingly, by the addition of dichloromethane or by the presence of their vapors, it is possible to break these intermolecular contacts allowing the recovery of the natural greenish emission.

Taking advantage of these mechano- and thermochromic properties of the pyrazolate Pt^{II} complexes we have developed stimuli-responsive polymer thin films doped with them. The PVP and PMMA polymer matrixes were suitable to achieve the molecular aggregation and, therefore, the mechanochromic response of the material.

Experimental Section

Starting Materials

All commercial chemicals were purchased from Sigma-Aldrich, Alfa-Aesar or Maybridge and used without further purification. The 3,5-*n*-dialkyloxyacetophenone compounds were synthesized by a Williamson alkylation as we reported in a previous work.[20]

Physical measurements

The elemental analyses (C, H, N) were carried out by the Microanalytical Service of Complutense University (validated range: %C 0.5 – 94.7, %H 0.5 – 7.6, %N 0.5 – 23.0). IR spectra were recorded on a FTIR Thermo Nicolet 200 spectrophotometer with samples as KBr pellets in the 4000 – 400 cm^{-1} region: w (weak), m (medium) and s (strong). ^{1}H and ^{13}C NMR, 2D COSY, selective 1D NOESY, ^{1}H-^{13}C HMQC and ^{1}H-^{13}C HMBC spectra were performed at room temperature on a Bruker DPX-300 spectrophotometer (NMR Service of Complutense University) from solutions in $CDCl_3$. Chemical shifts δ are listed relative to Me_4Si using the signal of the deuterated solvent as a reference (7.26 and 77.0 ppm for ^{1}H and ^{13}C, respectively) and coupling constants *J* are in hertz. Multiplicities are indicated as s (singlet), d (doublet), t (triplet), q (quartet), qt (quintet), ddd (doublet of doublets of doublets), m (multiplet), br (broad signal). The ^{1}H and ^{13}C chemical shifts are accurate to ±0.01 and ±0.1 ppm, respectively, and coupling constants to ±0.3 Hz.

Thermal studies were carried out by optical microscopy using an Olympus BX50 microscope equipped with a Linkam THMS 600 heating stage. The temperatures were assigned on the basis of optic observations with polarized light. Measurements of the transition temperatures and their associated enthalpies were made using a Perkin Elmer Pyris 1 differential scanning calorimeter with the sample (1 – 4 mg) sealed hermetically in aluminum pans and with a heating or cooling rate of 10 K min^{-1}. The X-ray diffractograms at variable temperature were recorded on a Panalytical X'Pert PRO MPD diffractometer with Cu-Kα (1.54 Å) radiation in a θ–θ configuration equipped with an Anton Paar HTK1200 heating stage (X-Ray Diffraction Service of Complutense University).

Photophysical measurements

UV-Vis absorption spectra were recorded on a Jasco V-650 spectrophotometer equipped with a Julabo thermostat, and the luminescence emission using a Horiba-Jobin-Yvon Fluoromax-4 spectrofluorimeter in the PROTEOMASS-BIOSCOPE Facilites. The linearity of the luminescence emission *vs*. concentration was checked in the concentration range used (10^{-5} – 10^{-6} M). A correction for the absorbed light was performed when necessary. The stock solutions of the ligands and complexes (*ca*. 10^{-3} M) were prepared by dissolving an appropriate amount of the corresponding compound in a 10 mL volumetric flask and diluting to the mark with dichloromethane. The studied solutions were prepared by appropriate dilution of the stock solutions up to 10^{-5} – 10^{-6} M. All measurements were performed at 298 K.

The relative luminescence quantum yields were determined using a solution of 2-aminopyridine in sulfuric acid (0.1 M) for ligands and other one of acridine yellow in absolute ethanol for Pt^{II} complexes as the

standards ($\Phi_{F(2\text{-aminopyridine})}$ = 0.60, $\Phi_{F(\text{acridine yellow})}$ = 0.47).[21] The lifetime measurement in degassed CH_2Cl_2 solution was performed with a Tempro Fluorescence Lifetime System, from Horiba J-Y (PROTEOMASS-BIOSCOPE Facilities).

Luminescence spectra of solid samples were recorded on the Horiba J-Y Fluoromax-4 spectrofluorimeter using a fiber-optics device connected to the spectrofluorimeter, exciting the solid compounds at appropriated λ [nm]. The emission spectra at variable temperature were recorded by heating the samples over a hotplate with an external temperature control provided with a XS instrument digital thermo par.

Synthesis of ligands 3-(3,5-bis(alkyloxy)phenyl)-5-(isoquinolin-3-yl)pyrazole, [Hpz$^{R(n,n)iq}$] a4-a18

A mixture of the corresponding 3,5-*n*-dialkyloxyacetophenone (2.05 mmol) and 60% NaH (8.19 mmol, 0.17 g) in 50 mL of dry THF was stirred for 1 h at room temperature. Then, ethyl isoquinoline-3-carboxylate (2.05 mmol, 0.41g) was slowly added and the reaction mixture refluxed for 24 h. After cooling the solution to room temperature, 10 mL of methanol were added to quench the excess of NaH and the solvent was removed to yield a brown residue, which was dissolved in ethyl acetate. The new solution was washed first with 30 mL of dilute HCl (2 M) and then with water (3 x 50 mL), being finally dried upon anhydrous magnesium sulphate. By evaporation of the solvent, a viscous oil corresponding to the β-diketone was obtained. Without further purification, a solution of hydrazine monohydrate (2.05 mmol, 0.10 g) in 15 mL of ethanol was slowly added to a solution of the corresponding β-diketone in the same solvent (50 mL). The mixture was heated at reflux for 24 h and then cooled at 4 ºC to induce precipitation. The pale yellow precipitate was recrystallized in THF/ethanol to give a white solid, which filtered off and dried *in vacuo* (38-61%, depending on the alkyl chain length).

All compounds were characterized by IR and ^{1}H NMR spectroscopies and elemental analysis (deposited in the Supporting Information). In addition, ligand **a4** was also characterized by ^{13}C NMR, and their analytical and spectroscopic data are shown below as a representative example.

[Hpz$^{R(4,4)iq}$] **(a4)**: ^{1}H NMR (300 MHz, $CDCl_3$, 25 ºC, TMS): δ = 0.99 (t, *J* = 7.4 Hz, 6H; CH_3), 1.24 (t, *J* = 7.0 Hz, EtOH), 1.51 (m, 4H, CH_2), 1.79 (qt, *J* = 6.6 Hz, 4H; CH_2), 3.73 (q, *J* = 7.0 Hz, EtOH), 4.03 (t, *J* = 6.5 Hz, 4H; OCH_2), 6.47 (t, *J* = 2.3 Hz, 1H; H_p), 7.03 (d, *J* = 2.2 Hz, 2H; H_o), 7.13 (s, 1H, 4'-H), 7.62 (dd, *J* = 8.0, 7.9 Hz, 1H; 7-H), 7.73 (dd, *J* = 8.0, 8.0 Hz, 1H; 6-H), 7.89 (d, *J* = 8.2 Hz, 1H; 5-H), 8.01 (d, *J* = 8.2 Hz, 1H; 8-H), 8.08 (s, 1H, 4-H), 9.28 (s, 1H, 1-H); ^{13}C NMR (75.48 MHz, $CDCl_3$, 25 ºC, TMS): δ = 13.8 (CH_3), 19.2 (CH_2), 31.4 (CH_2), 67.8 (OCH_2), 100.1 (C4'), 101.4 (C_P), 104.1 (C_o), 116.1 (C4), 126.9 (C5), 127.4 (C7), 127.8 (C8), 128.1 (C10), 131.0 (C6), 134.3 (C_i), 136.4 (C9), 142.2 (C3), 144.9 (C5'), 151.6 (C3'), 152.4 (C1), 160.6 (C_m); IR (KBr): ν = 3249 (m, ν(N–H)), 1621-1585 (m, ν(C=C + C=N)); elemental analysis calcd (%) for $C_{26}N_3H_{29}O_2 \cdot 0.3$EtOH: C 74.1, H 6.9, N 10.1; found: C 74.4, H 7.2, N 9.8.

Synthesis of complexes [Pt(pz$^{R(n,n)iq}$)$_2$] b4-b18

A solution of K_2PtCl_4 (0.24 mmol, 0.1 g) in 5 mL of distilled water was added over another solution of the corresponding pyrazole [Hpz$^{R(n,n)iq}$] (0.48 mmol) in 15 mL of ethanol. The mixture reaction was refluxed for 16 h and the solvent was then decanted to obtain a black residue which was dissolved in 5 mL of $CHCl_3$. The resulting solution was filtered through a pad of Celite and concentrated *in vacuo*. Addition of acetone gave the title Pt^{II} complexes as yellow solids (29-52%, depending on the alkyl chain length).

[Pt(pz$^{R(4,4)iq}$)$_2$] **(b4)**: ^{1}H NMR (300 MHz, $CDCl_3$, 25 ºC, TMS): δ = 1.11 (t, *J* = 7.3 Hz, 12H; CH_3), 1.60 (qt, *J* = 7.2 Hz, 8H; CH_2), 1.87 (qt, *J* = 6.6 Hz, 8H; CH_2), 3.91 (t, *J* = 6.6 Hz, 8H; OCH_2), 6.17 (s, 2H, 4'-H), 6.31 (br, 2H, H_p), 6.53 (br, 4H, H_o), 7.04 (s, 2H, 4-H), 7.18 (m, 2H, 7-H), 7.18 (m, 2H, 5-H), 7.39 (br, 2H, 8-H), 7.47 (br, 2H ,6-H), 10.80 (s, 2H, 1-H); IR (KBr): ν = 1641-1599 (s, ν(C=C + C=N)); elemental analysis calcd (%) for $PtC_{52}N_6H_{56}O_4$: C 61.0, H 5.5, N 8.2; found: C 60.6, H 5.4, N 8.3.

[Pt(pz$^{R(6,6)iq}$)$_2$] **(b6)**: ^{1}H NMR (300 MHz, $CDCl_3$, 25 ºC, TMS): δ = 1.01 (t, *J* = 6.9 Hz, 12H; CH_3), 1.47 (m, 24H, CH_2), 1.86 (qt, *J* = 6.8 Hz, 8H; CH_2), 3.85 (t, *J* = 6.5 Hz, 8H; OCH_2), 6.06 (s, 2H, 4'-H), 6.29 (br, 2H, H_p), 6.49 (br, 4H, H_o), 6.93 (s, 2H, 4-H), 7.14 (m, 2H, 7-H), 7.14 (m, 2H, 5-H), 7.28 (d, *J* = 8.2 Hz, 2H, 8-H), 7.45 (dd, *J* = 7.5, 7.5 Hz, 2H; 6-H), 10.71 (s, 2H, 1-H); IR (KBr): ν = 1640-1596 (s, ν(C=C + C=N)); elemental analysis calcd (%) for $PtC_{60}N_6H_{72}O_4 \cdot H_2O$: C 62.4, H 6.5, N 7.3; found: C 62.3, H 6.2, N 7.4.

[Pt(pz$^{R(8,8)iq}$)$_2$] **(b8)**: ^{1}H NMR (300 MHz, $CDCl_3$, 25 ºC, TMS): δ = 0.96 (t, *J* = 6.7 Hz, 12H; CH_3), 1.38 (m, 40H, CH_2), 1.87 (qt, *J* = 6.6 Hz, 8H; CH_2), 3.86 (t, *J* = 6.7 Hz, 8H; OCH_2), 6.10 (s, 2H, 4'-H), 6.30 (t, *J* = 2.2 Hz, 2H; H_p), 6.52 (d, *J* = 2.2 Hz, 4H; H_o), 6.96 (s, 2H, 4-H), 7.16 (m, 2H, 7-H), 7.16 (m, 2H, 5-H), 7.32 (d, *J* = 8.1 Hz, 2H; 8-H), 7.47 (dd, *J* = 7.5, 7.5 Hz, 2H; 6-H), 10.76 (s, 2H, 1-H); IR (KBr): ν = 1640-1595 (s, ν(C=C + C=N)); elemental analysis calcd (%) for $PtC_{68}N_6H_{88}O_4 \cdot H_2O$: C 64.5, H 7.2, N 6.6; found: C 64.9, H 6.9, N 6.8.

[Pt(pz$^{R(10,10)iq}$)$_2$] **(b10)**: ^{1}H NMR (300 MHz, $CDCl_3$, 25 ºC, TMS): δ = 0.92 (t, *J* = 6.8 Hz, 12H; CH_3), 1.34 (m, 56H, CH_2), 1.88 (qt, *J* = 7.2 Hz, 8H; CH_2), 3.92 (t, *J* = 6.7 Hz, 8H; OCH_2), 6.26 (s, 2H, 4'-H), 6.34 (br, 2H, H_p), 6.64 (br, 4H, H_o), 7.13 (s, 2H, 4-H), 7.26 (m, 2H, 7-H), 7.26 (m, 2H, 5-H), 7.47 (d, *J* = 8.2 Hz, 2H; 8-H), 7.53 (dd, *J* = 7.7, 7.7 Hz, 2H; 6-H), 10.92 (s, 2H, 1-H); IR (KBr): ν = 1640-1596 (s, ν(C=C + C=N)); elemental analysis calcd (%) for $PtC_{76}N_6H_{104}O_4 \cdot H_2O$: C 66.2, H 7.7, N 6.1; found: C 66.3, H 7.5, N 6.2.

[Pt(pz$^{R(12,12)iq}$)$_2$] **(b12)**: ^{1}H NMR (300 MHz, $CDCl_3$, 25 ºC, TMS): δ = 0.91 (t, *J* = 6.9 Hz, 12H; CH_3), 1.31 (m, 72H, CH_2), 1.87 (qt, *J* = 7.3 Hz, 8H; CH_2), 3.87 (t, *J* = 6.7 Hz, 8H; OCH_2), 6.14 (s, 2H, 4'-H), 6.31 (br, 2H, H_p), 6.56 (br, 4H, H_o), 7.01 (s, 2H, 4-H), 7.19 (m, 2H, 7-H), 7.19 (m, 2H, 5-H), 7.37 (d, *J* = 7.8 Hz, 2H; 8-H), 7.49 (dd, *J* = 7.5, 7.5 Hz, 2H; 6-H), 10.81 (s, 2H, 1-H); IR (KBr): ν = 1640-1597 (s, ν(C=C + C=N)); elemental analysis calcd (%) for $PtC_{84}N_6H_{120}O_4 \cdot H_2O$: C 67.7, H 8.2, N 5.6; found: C 67.9, H 7.9, N 5.6.

[Pt(pz$^{R(14,14)iq}$)$_2$] **(b14)**: ^{1}H NMR (300 MHz, $CDCl_3$, 25 ºC, TMS): δ = 0.90 (t, *J* = 6.8 Hz, 12H; CH_3), 1.30 (m, 88H, CH_2), 1.88 (qt, *J* = 7.2 Hz, 8H; CH_2), 3.87 (t, *J* = 6.8 Hz, 8H; OCH_2), 6.13 (s, 2H, 4'-H), 6.31 (br, 2H, H_p), 6.55 (br, 4H, H_o), 7.00 (s, 2H, 4-H), 7.18 (m, 2H, 7-H), 7.18 (m, 2H, 5-H), 7.34 (br, 2H, 8-H), 7.49 (br, 2H, 6-H), 10.79 (s, 2H, 1-H); ^{13}C NMR (75.48 MHz, $CDCl_3$, 25 ºC, TMS): δ = 14.1, 22.7, 26.4, 29.4, 29.8, 29.9, 32.0, 67.7, 98.1, 99.4, 102.1, 113.2, 125.7, 125.9, 126.2, 128.5, 131.2, 135.8, 136.8, 146.4, 148.2, 149.9, 155.0, 159.8; IR (KBr): ν = 1640-1598 (m, ν(C=C + C=N)); elemental analysis calcd (%) for $PtC_{92}N_6H_{136}O_4$: C 69.7, H 8.6, N 5.3; found: C 69.3, H 8.4, N 5.3.

[Pt(pz$^{R(16,16)iq}$)$_2$] **(b16)**: ^{1}H NMR (300 MHz, $CDCl_3$, 25 ºC, TMS): δ = 0.88 (t, *J* = 6.8 Hz, 12H; CH_3), 1.28 (m, 104H, CH_2), 1.89 (qt, *J* = 7.3 Hz, 8H; CH_2), 3.94 (t, *J* = 6.7 Hz, 8H; OCH_2), 6.31 (s, 2H, 4'-H), 6.35 (br, 2H, H_p), 6.68 (br, 4H, H_o), 7.18 (s, 2H, 4-H), 7.29 (m, 2H, 7-H), 7.29 (m, 2H, 5-H), 7.53 (m, 2H, 8-H), 7.53 (m, 2H, 6-H), 11.00 (s, 2H, 1-H); IR (KBr): ν = 1641-1598 (m, ν(C=C + C=N)); elemental analysis calcd (%) for $PtC_{100}N_6H_{152}O_4 \cdot H_2O$: C 70.0, H 9.0, N 4.9; found: C 70.2, H 8.8, N 5.1.

[Pt($pz^{R(18,18)iq}$)$_2$] **(b18)**: ^{1}H NMR (300 MHz, $CDCl_3$, 25 ºC, TMS): δ = 0.88 (t, J = 6.9 Hz, 12H; CH_3), 1.27 (m, 120H, CH_2), 1.88 (m, 8H, CH_2), 3.97 (br, 8H, OCH_2), 6.37 (s, 2H, 4'-H), 6.46 (br, 2H, H_p), 6.77 (br, 4H, H_o), 7.26 (s, 2H, 4-H), 7.34 (m, 2H, 7-H), 7.34 (m, 2H, 5-H), 7.60 (m, 2H, 8-H), 7.60 (m, 2H, 6-H), 11.12 (s, 2H, 1-H); IR (KBr): ν = 1640-1598 (m, ν(C=C + C=N)); elemental analysis calcd (%) for $PtC_{108}N_6H_{168}O_4{\cdot}H_2O$: C 71.0, H 9.4, N 4.7; found: C 70.8, H 9.0, N 4.8.

Fabrication of the stimuli-responsive polymer films

The polymer thin films based on polymethylmethacrylate (PMMA) and polyvinylpyrrolidone (PVP) were obtained from a solution of the polymer (100 mg) and the corresponding complex (1 mg) in *ca.* 20 mL of dichloromethane, followed by a slow evaporation of the solvent at room temperature (~ 24 h).

DFT Calculations

DFT calculations were run with Gaussian 03W software package[22] and the results were visualized by using Gauss-View.[23] The molecular structure of the Pt^{II} complex was optimized using the B3LYP level and the LanL2DZ basis set, which provides a D95V set for hydrogen and first-row elements and a Los Alamos ECP plus DZ set for the platinum atom. The terminal alkyl chains were replaced by methyl groups in order to reduce the calculation times. The natural bond orbital (NBO) atomic charges were determined from the optimized structure.

Acknowledgements

M. Cano thanks the Spanish Ministerio de Economía y Competitividad (project CTQ2011-25172) and Complutense University (GR3/14-910300), for funding. C. Cuerva acknowledges the Universidad Complutense de Madrid for his predoctoral contract (Programa de Financiación de Universidad Complutense de Madrid-Santander Universidades) and the financial help for international attendances. This work was supported by the Unidade de Ciências Biomoleculares Aplicadas-UCIBIO which are financed by national funds from FCT/MEC (UID/Multi/04378/2013) and co-financed by the ERDF under the PT2020 Partnership Agreement. CL is grateful to the Scientific Society PROTEOMASS (Portugal) for funding and facilities. We also wish to thank Dra. Elisabete Oliveira for her technical assistance with the luminescence measurements.

Keywords: platinum • liquid crystals • metallomesogens • smart materials • sensors

[1] a) A. Pucci, G. Ruggeri, *J. Mater. Chem.* **2011**, *21*, 8282-8291; b) Z. Chi, X. Zhang, B. Xu, X. Zhou, C. Ma, Y. Zhang, S. Liu, J. Xu, *Chem. Soc. Rev.* **2012**, *41*, 3878-3896; c) K. Ariga, T. Mori, J. P. Hill, *Adv. Mater.* **2012**, *24*, 158-176.

[2] a) X.-Q. Wang, C.-F. Wang, Z.-F. Zhou, S. Chen, *Adv. Opt. Mater.* **2014**, *2*, 652-662; b) Y. Sagara, T. Komatsu, T. Ueno, K. Hanaoka, T. Kato, T. Nagano, *Adv. Funct. Mater.* **2013**, *23*, 5277-5284; c) F. Ciardelli, G. Ruggeri, A. Pucci, *Chem. Soc. Rev.* **2013**, *42*, 857-870; d) S. Herrmann, J. T. Margraf, T. Clarck, C. Streb, *Chem. Commum.* **2015**, *51*, 13702-13705.

[3] a) R. Thirumalai, R. D. Mukhopadhyay, V. K. Praveen, A. Ajayaghosh, *Sci. Rep.* **2015**, *5*:9842; b) B. Yoon, D.-Y. Ham, O. Yarimaga, H. An, C. W. Lee, J.-M. Kim, *Adv. Mater.* **2011**, *23*, 5492-5497.

[4] H. Sun, S. Liu, W. Lin, K. Y. Zhang, W. Lv, X. Huang, F. Huo, H. Yang, G. Jenkins, Q. Zhao, W. Huang, *Nat. Commun.* **2014**, *5*:3601.

[5] a) X. Hou, C. Ke, C. J. Bruns, P. R. McGonigal, R. B. Pettman, J. F. Stoddart, *Nat. Commun.* **2015**, *6*:6884; b) X. Zhu, R. Liu, Y. Li, H. Huang, Q. Wang, D. Wang, X. Zhu, S. Liu, H. Zhu, *Chem. Commun.* **2014**, *50*, 12951-12954.

[6] a) W. B. Connick, R. E. Marsh, W. P. Schaefer, H. B. Gray, *Inorg. Chem*. **1997**, *36*, 913-922; b) V. W.-W.Yam, K. M.-C. Wong, N. Zhu, *J. Am. Chem. Soc.* **2002**, *124*, 6506-6507; c) T. Kayano, S. Takayasu, K. Sato, K. Shinozaki, *Chem. Eur. J.* **2014**, *20*, 16583-16589; d) M. R. R. Prabhath, J. Romanova, R. J. Curry, S. R. P. Silva, P. D. Jarowski, *Angew. Chem. Int. Ed.* **2015**, *54*, 7949-7953; e) Y. Chen, C.-M. Che, W. Lu, *Chem. Commun.* **2015**, *51*, 5371-5374; f) K. Li, G. S. M. Tong, Q. Wan, G. Cheng, W.-Y. Tong, W.-H. Ang, W.-L. Kwong, C.-M. Che, *Chem. Sci.* **2016**, *7*, 1653-1673; g) K. M.-C. Wong, V. W.-W. Yam, *Acc. Chem. Res.* **2011**, *44*, 424-434; h) V. W.-W. Yam, V. K.-M. Au, S. Y.-L. Leung, *Chem. Rev.* **2015**, 115, 7589-7728.

[7] a) S.-B. Ko, H.-J. Park, S. Gong, X. Wang, Z.-H. Lu, S. Wang, *Dalton Trans.* **2015**, *44*, 8433-8443; b) B. Wang, F. Liang, H. Hu, Y. Liu, Z. Kang, L.-S. Liao, J. Fan, *J. Mater. Chem. C* **2015**, *3*, 8212-8218; c) T. Tanaka, R. Nouchi, Y. Nakao, Y. Arikawa, K. Umakoshi, *RSC Adv.* **2014**, *4*, 62186-62189; d) A. I. Solomatina, D. V. Krupenya, V. V. Gurzhiy, I. Zlatkin, A. P. Pushkarev, M. N. Bochkarev, N. A. Besley, E. Bichoutskaia, S. P. Tunik, *Dalton Trans.* **2015**, *44*, 7152-7162.

[8] S.-Y. Chang, J. Kavitha, S.-W. Li, C.-S. Hsu, Y. Chi, Y.-S. Yeh, P.-T. Chou, G.-H. Lee, A. J. Carty, Y.-T. Tao, C.-H. Chien, *Inorg. Chem.* **2006**, *45*, 137-146.

[9] a) C.-T. Liao, H.-H. Chen, H.-F. Hsu, A. Poloek, H.-H. Yeh, Y. Chi, K.-W. Wang, C.-H. Lai, G.-H. Lee, C.-W. Shih, P.-T. Chou, *Chem. Eur. J.* **2011**, *17*, 546-556; b) A. Díez, J. Forniés, C. Larraz, E. Lalinde, J. A. López, A. Martín, M. T. Moreno, V. Sicilia, *Inorg. Chem.* **2010**, *49*, 3239-3251; c) J. A. G. Williams, A. Beeby, E. S. Davies, J. A. Weinstein, C. Wilson, *Inorg. Chem.* **2003**, *42*, 8609-8611; d) V. V. Sivchik, E. V. Grachova, A. S. Melnikov, S. N. Smirnov, A. Yu. Ivanov, P. Hirva, S. P. Tunik, I. O. Koshevoy, *Inorg. Chem.* **2016**, *55*, 3351-3363; e) V. H. Houlding, V. M. Miskowski, *Coord. Chem. Rev.* **1991**, *111*, 145-152; f) J. A. Bailey, V. M. Miskowski, H. B. Gray, *Inorg. Chem.* **1993**, *32*, 369-370; g) J. A. Bailey, M. G. Hill, R. E. Marsh, V. M. Miskowski, W. P. Schaefer, H. B. Gray, *Inorg. Chem.* **1995**, *34*, 4591-4599; h) V. M. Miskowski, V. H. Houlding, *Inorg. Chem.* **1991**, *30*, 4446-4452; i) A. Y.-Y. Tam, K. M.-C. Wong, V. W.-W. Yam, *J. Am. Chem. Soc.* **2009**, *131*, 6253-6260.

[10] a) C. Cuerva, J. A. Campo, P. Ovejero, M. R. Torres, E. Oliveira, S. M. Santos, C. Lodeiro, M. Cano, *J. Mater. Chem. C* **2014**, *2*, 9167-9181; b) Y. Chen, W. Lu, C.-M. Che, *Organometallics* **2013**, *32*, 350-353; c) N. K. Allampally, C.-G. Daniliuc, C. A. Strssert, L. De Cola, *Inorg. Chem.* **2015**, *54*, 1588-1596; d) C. E. Buss, K. R. Mann, *J. Am. Chem. Soc.* **2002**, *124*, 1031-1039; e) A. G. Dylla, D. E. Janzen, M. K. Pomije, K. R. Mann, *Organometallics* **2007**, *26*, 6243-6247.

[11] M. Krikorian, S. Liu, T. Swager, *J. Am. Chem. Soc.* **2014**, *136*, 2952-2955.

[12] a) H.-Y. Ku, B. Tong, Y. Chi, H.-C. Kao, C.-C. Yeh, C.-H. Chang, G.-H. Lee, *Dalton Trans.* **2015**, *44*, 8552-8563; b) L.-M. Huang, G.-M. Tu, Y. Chi, W.-Y. Hung, Y.-C. Song, M.-R. Tsenq, P.-T. Chou, G.-H. Lee, K.-T. Wong, S.-H. Cheng, W.-S. Tsai, *J. Mater. Chem. C* **2013**, *1*, 7582-7592; c) C. Cuerva, J. A. Campo, M. Cano, B. Arredondo, B. Romero, E. Otón, J. M. Otón, *New J. Chem.* **2015**, *39*, 8467-8473.

[13] a) J. Ni, X. Zhang, N. Qiu, Y.-H. Wu, L.-Y. Zhang, J. Zhang, Z.-N. Chen, *Inorg. Chem.* **2011**, *50*, 9090-9096; b) X. Zhang, J.-Y. Wang, J. Ni, L.-Y. Zhang, Z.-N. Chen, *Inorg. Chem.* **2012**, *51*, 5569-5579.

[14] a) N. Kitani, N. Kuwamura, T. Tsukuda, N. Yoshinari, T. Konno, *Chem. Commun.* **2014**, *50*, 13529-13532; b) A. Han, P. Du, Z. Sun, H. Wu, H.

Jia, R. Zhang, Z. Liang, R. Cao, R. Eisenberg, *Inorg. Chem.* **2014**, *53*, 3338-3344; c) S. J. Choi, J. Kuwabara, Y. Nishimura, T. Arai, T. Kanbara, *Chem. Lett.* **2012**, *41*, 65-67; d) X.-P. Zhang, J.-F. Mei, J.-C. Lai, C.-H. Li, X.-Z. You, *J. Mater. Chem. C* **2015**, *3*, 2350-2357.

[15] a) X. Zhang, Z. Chi, Y. Zhang, S. Liu, J. Xu, *J. Mater. Chem. C* **2013**, *1*, 3376-3390; b) D. A. Davis, A. Hamilton, J. Yang, L. D. Cremar, D. Van Gough, S. L. Potisek, M. T. Ong, P. V. Braun, T. J. Martínez, S. R. White, J. S. Moore, N. R. Sottos, *Nature* **2009**, *459*, 68-72; c) J. R. Kumpfer, S. D. Taylor,W. B. Connick, S. J. Rowan, *J. Mater. Chem.* **2012**, *22*, 14196-14204; d) D. Yang, S. Ye, J. Ge, *Adv. Funct. Mater.* **2014**, *24*, 3197-3205; e) N. Mizoshita, T. Tani, S. Inagaki, *Adv. Mater.* **2012**, *24*, 3350-3355; f) Y. Sagara, T. Kato, *Angew. Chem. Int. Ed.* **2011**, *50*, 9128-9132; g) S. Yamane, Y. Sagara, T. Mutai, K. Araki, T. Kato, *J. Mater. Chem. C* **2013**, *1*, 2648-2656; h) J. Sun, X. Lv, P. Wang, Y. Zhang, Y. Dai, Q. Wu, M. Ouyang, C. Zhang, *J. Mater. Chem. C* **2014**, *2*, 5365-5371; i) M. Mitani, S. Ogata, S. Yamane, M. Yoshio, M. Hasegaw, T. Kato, *J. Mater. Chem. C* **2016**, *4*, 2752-2760; j) J. R. Kumpfer, S. D. Taylor, W. B. Connick, S. J. Rowan, *J. Mater. Chem.* **2012**, *22*, 14196-14204; k) S. D. Taylor, A. E. Norton, R. T. Hart Jr., M. K. Abdolmaleki, J. A. Krause, W. B. Connick, *Chem. Commun.* **2013**, *49*, 9161-9163; l) S. M. Drew, L. I. Smith, K. A. McGee, K. R. Mann, *Chem. Mater.* **2009**, *21*, 3117-3124; m) D. E. Janzen, K. R. Mann, *Dalton Trans.* **2015**, *44*, 4223-4237.

[16] a) V. N. Kozhevnikov, B. Donnio, D. W. Bruce, *Angew. Chem. Int. Ed.* **2008**, *47*, 6286-6289; b) K. Binnemans, *J. Mater. Chem.* **2009**, *19*, 448-453; c) Y. Molard, F. Dorson, V. Cîrcu, T. Roisnel, F. Artzner, S. Cordier, *Angew. Chem. Int. Ed.* **2010**, *49*, 3351-3355; d) A. Santoro, A. M. Prokhorov, V. N. Kozhevnikov, A. C. Whitwood, B. Donnio, J. A. G. Williams, D. W. Bruce, *J. Am. Chem. Soc.* **2011**, 133, 5248-5251; e) S.-T. Lam, V. W.-W. Yam, *Chem. Eur. J.* **2010**, *16*, 11588-11593; f) R. Chico, E. Castillejos, P. Serp, S. Coco, P. Espinet, *Inorg. Chem.* **2011**, *50*, 8654-8662.

[17] A. Aliprandi, D. Genovese, M. Mauro, L. De Cola, *Chem. Lett.* **2015**, *44*, 1152-1169.

[18] T. Komatsu, K. Ohta, T. Watanabe, H. Ikemoto, T. Fujimoto, I. Yamamoto, *J. Mater. Chem.* **1994**, *4*, 537-540.

[19] S.-Y. Chang, J. Kavitha, J.-Y. Hung, Y. Chi, *Inorg. Chem.* **2007**, *46*, 7064-7074.

[20] C. Cuerva, J. A. Campo, P. Ovejero, M. R. Torres, M. Cano, *Dalton Trans.* **2014**, *43*, 8849-8860.

[21] I. B. Berlman, *Handbook of Fluorescence Spectra of Aromatic Molecules*, Academic Press, New York, USA 1971.

[22] M. J. Frisch, G. W. Trucks, H. B. Schlegel, G. E. Scuseria, M. A. Robb, J. R. Cheeseman, G. Scalmani, V. Barone, B. Mennucci, G. A. Petersson, H. Nakatsuji, M. Caricato, X. Li, H. P. Hratchian, A. F. Izmaylov, J. Bloino, G. Zheng, J. L. Sonnenberg, M. Hada, M. Ehara, K. Toyota, R. Fukuda, J. Hasegawa, M. Ishida, T. Nakajima, Y. Honda, O. Kitao, H. Nakai, T. Vreven, J. A. Montgomery, Jr., J. E. Peralta, F. Ogliaro, M. Bearpark, J. J. Heyd, E. Brothers, K. N. Kudin, V. N. Staroverov, R. Kobayashi, J. Normand, K. Raghavachari, A. Rendell, J. C. Burant, S. S. Iyengar, J. Tomasi, M. Cossi, N. Rega, J. M. Millam, M. Klene, J. E. Knox, J. B. Cross, V. Bakken, C. Adamo, J. Jaramillo, R. Gomperts, R. E. Stratmann, O. Yazyev, A. J. Austin, R. Cammi, C. Pomelli, J. W. Ochterski, R. L. Martin, K. Morokuma, V. G. Zakrzewski, G. A. Voth, P. Salvador, J. J. Dannenberg, S. Dapprich, A. D. Daniels, Ö. Farkas, J. B. Foresman, J. V. Ortiz, J. Cioslowski, D. J. Fox, Gaussian 03, Revision E.01, Gaussian Inc, Wallingford, Conn, USA, 2004.

[23] R. Dennington II, T. Keith, J. Millam, Gauss View, Semichem Inc., Shawnee Mission, Kan, USA, 2007.

Entry for the Table of Contents

FULL PAPER

Stimuli-responsive luminescent Pt^{II} metallomesogens are synthesized and used as dopant agents in the fabrication of smart polymer thin films. The high planar geometry of these complexes favors aggregation-induced emission, which can be controlled by applying of external stimuli such as heat, pressure or mechanical grinding.

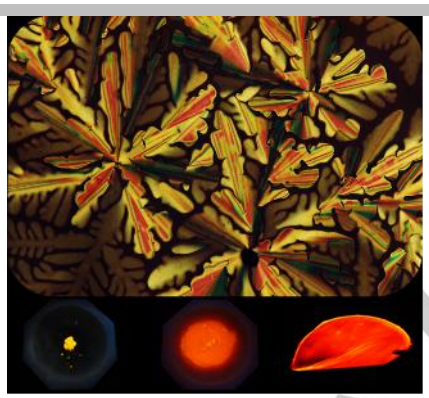

Cristián Cuerva, José A. Campo, Mercedes Cano, and Carlos Lodeiro**

Page No. – Page No.

Platinum(II) Metallomesogens, New External Stimuli-Responsive Photoluminescence Materials